Supplementary Materials for

Structural composition of antibacterial zinc-doped geopolymers

Xiaojuan Kang, and Hailong Ye*

Department of Civil Engineering, The University of Hong Kong, Pokfulam, Hong Kong, China

*Corresponding author, Email: hlye@hku.hk

This file includes:

Figures S1 to S7

Tables S1 to S7

Materials

MK precursor is largely amorphous with a small amount of anatase and quartz, and the MK particles have an intermediate particle size (D_{50}) of ~10.9 μm, with an empirical formula of $2SiO_2 \cdot Al_2O_3$ (Si/Al molar ratio=1.0). Nano zinc oxide (NanoTek, Alfa Aesar) is a powder with a particle size of 40-100 nm and a surface area of 10-25 m^2/g. All chemicals in this experiment are analytically pure with the details as follows: sodium hydroxide powder (Uni-Chem, 99% purity, NaOH), sodium silicate solution (Uni-Chem) with the detailed composition as shown in Table S2, zinc nitrate (DUKSAN, extra pure).

Table S1 Oxide composition of unreacted MK precursor determined by XRF.

Sample	SiO_2	Al_2O_3	TiO_2	P_2O_5	Na_2O	Fe_2O_3	MgO	CaO	K_2O	LOI
GGBS	52.57	44.38	0.822	0.692	0.487	0.420	0.193	0.145	0.106	0.46

Note: LOI refers to the loss on ignition, as measured at 950 °C for 1 h by a thermogravimetric analyser.

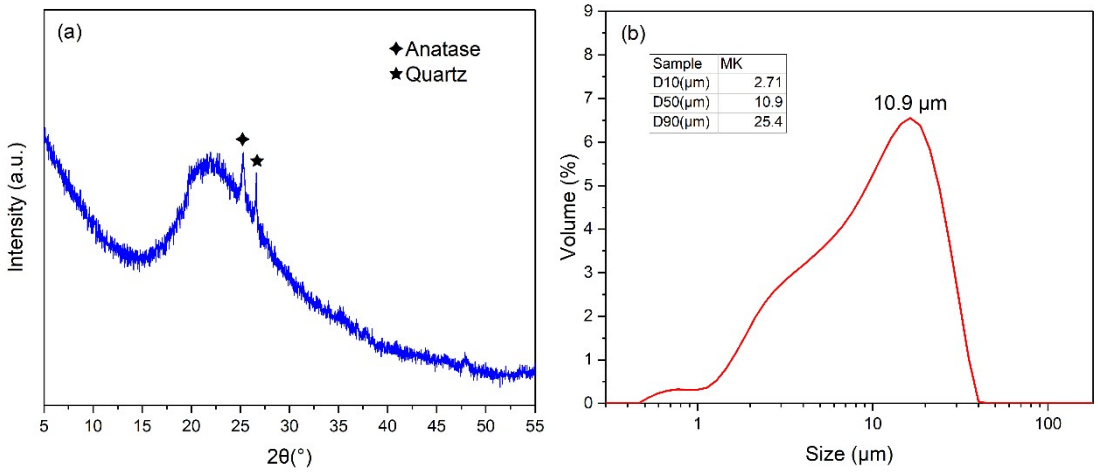

Figure S1 a) XRD diffractogram of unreacted MK precursor. b) Particle size distribution of MK determined by dynamic light scattering.

Table S2 Chemical composition of sodium silicate solution.

Chemical	Na_2O/ wt.%	SiO_2/wt.%	Water content / wt.%
Sodium silicate	12	30	58

Microbial corrosion setup

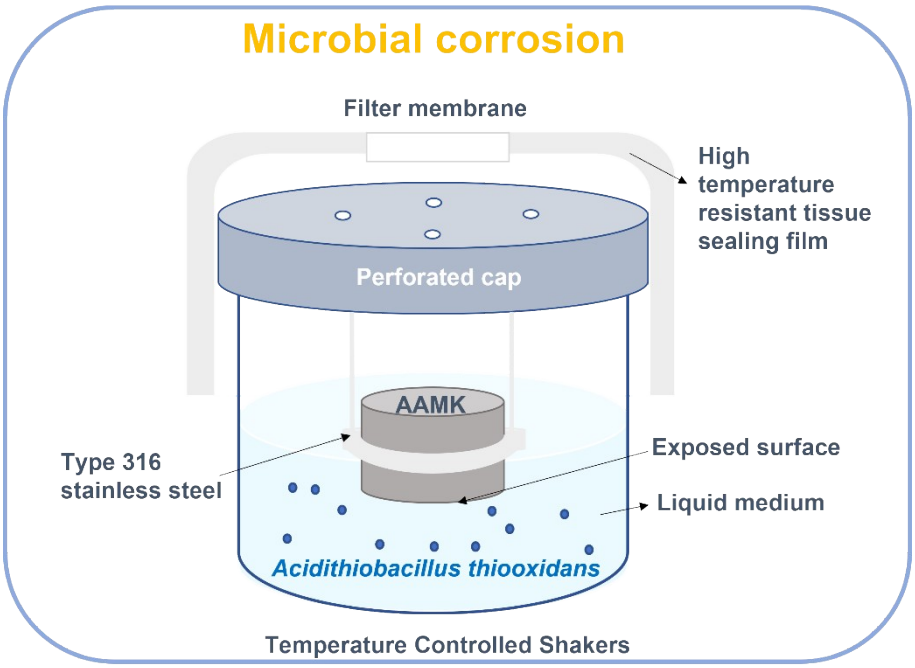

Figure S2 Setup of microbial corrosion test.

SEM images for Fig. 1f in the manuscript

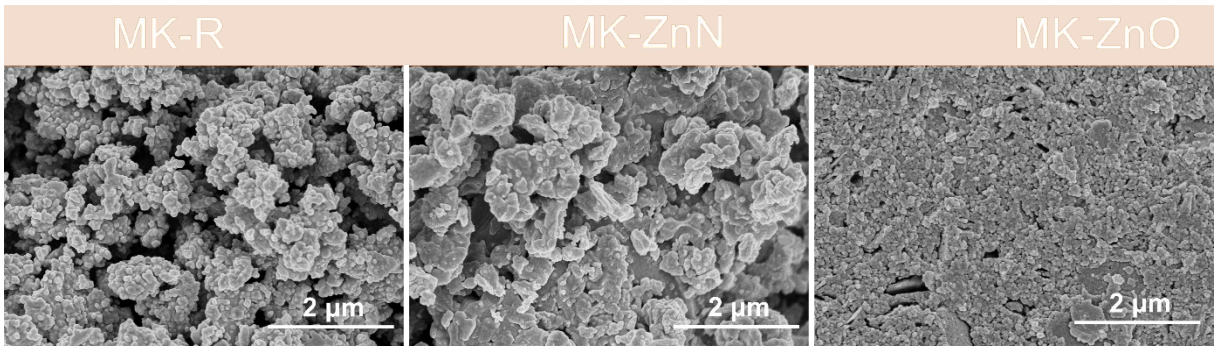

Figure S3 SEM images of Zn-doping AAMK geopolymers.

NMR data

Tables S3-S5 are for Table 1 in manuscript.

Table S3 Parameter statistics of the deconvoluted ^{29}Si MAS NMR spectra in R.

R	Integral area	Relative integral areas /%
$Q^4(4Al)$	$(1.31\pm0.21)\times10^9$	10.6
$Q^4(3Al)$	$(1.72\pm1.00)\times10^9$	14.0
$Q^4(2Al)$	$(2.93\pm1.50)\times10^9$	23.8
$Q^4(1Al)$	$(1.35\pm0.82)\times10^9$	11.0
$Q^4(0Al)$	$(5.12\pm0.15)\times10^9$	40.5

Table S4 Parameter statistics of the deconvoluted ^{29}Si MAS NMR spectra in ZnN-AAMK.

ZnN-AAMK	Integral area	Relative integral areas /%
$Q^4(4Al)$	$(1.48\pm1.17)\times10^9$	12.5
$Q^4(3Al)$	$(2.03\pm4.10)\times10^9$	17.4
$Q^4(2Al)$	$(2.13\pm5.02)\times10^9$	18.3
$Q^4(1Al)$	$(0.98\pm2.00)\times10^9$	8.4
$Q^4(0Al)$	$(4.91\pm0.26)\times10^9$	43.5

Table S5 Parameter statistics of the deconvoluted ^{29}Si MAS NMR spectra in ZnO-AAMK.

ZnO-AAMK	Integral area	Relative integral areas /%
$Q^4(4Al)$	$(1.51\pm0.22)\times10^9$	25.7
$Q^4(3Al)$	$(2.57\pm0.68)\times10^9$	42.3
$Q^4(2Al)$	$(1.55\pm0.80)\times10^9$	25.7
$Q^4(1Al)$	$(3.23\pm3.71)\times10^8$	5.4
$Q^4(0Al)$	$(5.30\pm4.20)\times10^7$	0.9

Table S6 The isotropic chemical shift and normalized relative integral areas for $Q^4(mAl)$

environments within each sample extracted from the deconvoluted ^{29}Si MAS NMR spectra.

The detailed data for Fig. 2f.

Samples	Fractions of silicon present in different tetrahedral environments					Reaction degree /%	Bound water /%
Q^n(mAl)/%	Q^4(4Al)	Q^4(3Al)	Q^4(2Al)	Q^4(1Al)	Q^4(0Al)	-	-
1	13.1	15.2	13.6	8.8	49.2	50.8	11.0
2	14.4	13.9	12.0	7.7	52.0	48.0	10.0
3	16.3	18.1	10.0	8.2	47.4	52.6	10.5
4	14.4	13.3	15.0	6.1	51.2	48.8	10.4
5	16.0	12.1	14.8	7.4	49.7	50.4	10.3
6	10.6	14.0	23.8	11.0	40.5	59.5	13.2
7	12.5	17.4	18.3	8.4	43.5	56.5	12.1
8	16.0	14.8	17.4	13.8	38.0	62.0	11.9
9	25.8	42.3	25.7	5.4	0.9	99.1	18.8
10	28.6	42.1	17.1	9.7	2.5	97.5	19.1

XAFS data

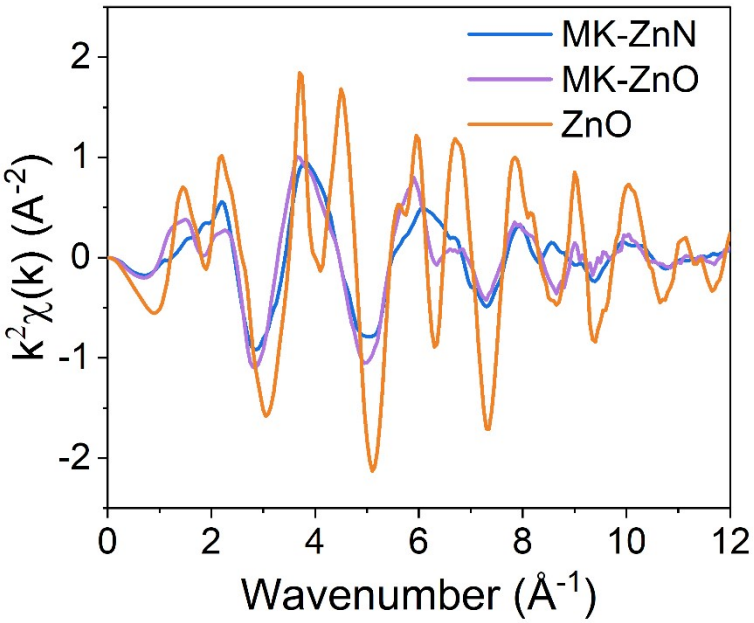

Figure S4 k^3-weighted Zn K-edge EXAFS spectra (χ function) of Zn-doping AAMK.

Fig. S4 displays k^3-weighted EXAFS spectra and. The ZnO crystal spectrum show stronger sinusoidal oscillation comparing with Zn-containing AAMK spectra, resulting from highly ordering of Zn environment in crystal.

Antibacterial properties and phase evaluation of MK-based geopolymer after microbial corrosion (MC)

Table S7 The isotropic chemical shift and normalised relative integral areas for Q^4(mAl) environments within each sample extracted from the deconvoluted ^{29}Si MAS NMR spectra. The detailed data for Fig. 5b and 5d.

	Fractions of silicon present in different tetrahedral environments					Si/Al ratio	Increase percentage
Q^n(mAl)/%	Q^4(4Al)	Q^4(3Al)	Q^4(2Al)	Q^4(1Al)	Q^4(0Al)	-	-
Chemical shift /ppm	-84.9	-90.8	-95.5	-100.6	-108.1	-	-
R-non-MC	10.6	14.0	23.8	11.0	40.5	1.7	-
R-MC	3.9	18.3	26.1	24.2	27.6	2.0	17.6%
MK-ZnO-non-MC	25.8	42.3	25.7	5.4	0.9	1.4	-
MK-ZnO-MC	23.6	38.9	20.8	13.1	3.6	1.5	7.1%

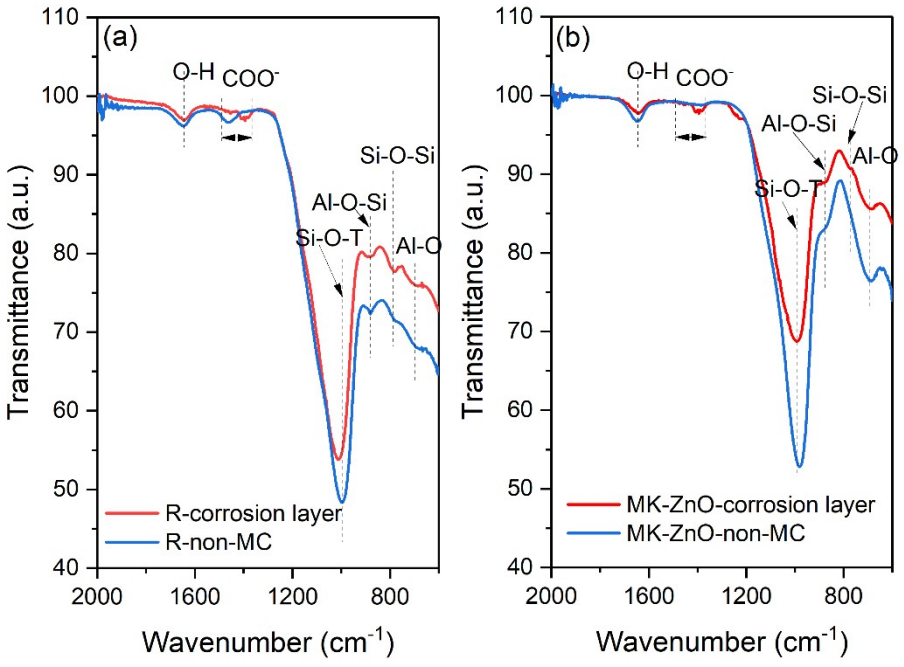

Figure S5 FTIR results of corrosion layer and non-MC samples of a) R and b) ZnO-AAMK.

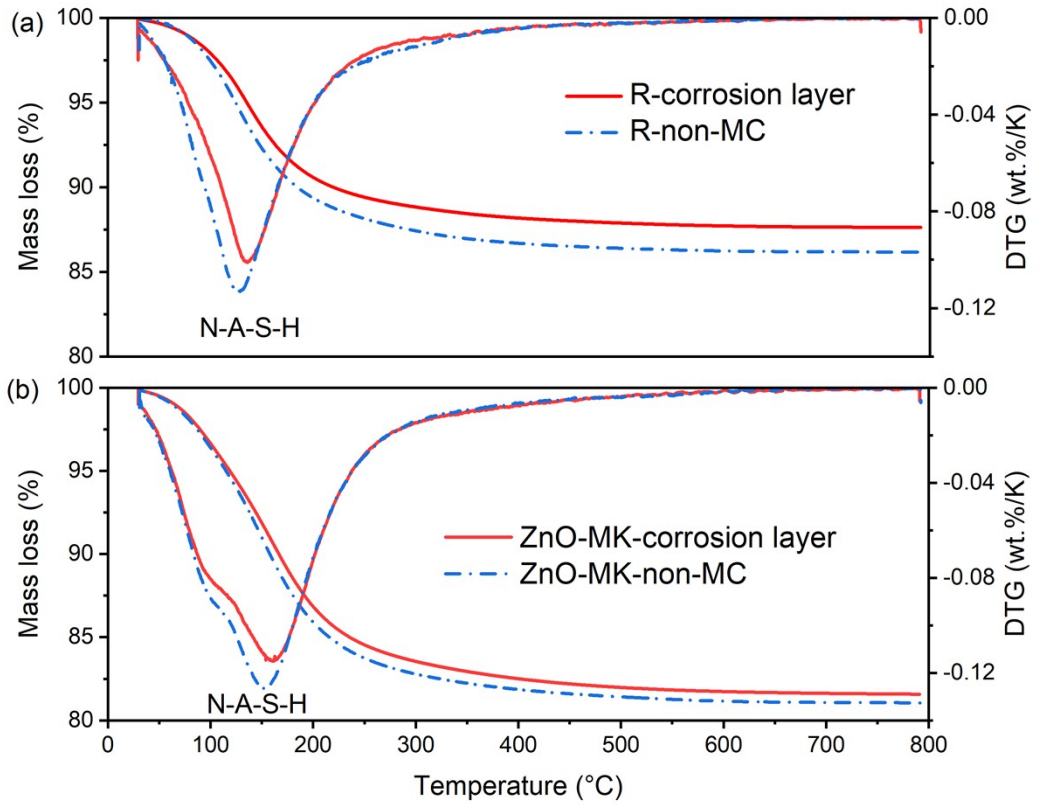

Figure S6 TGA results of corrosion layer and non-MC samples of a) R and b) ZnO-AAMK.

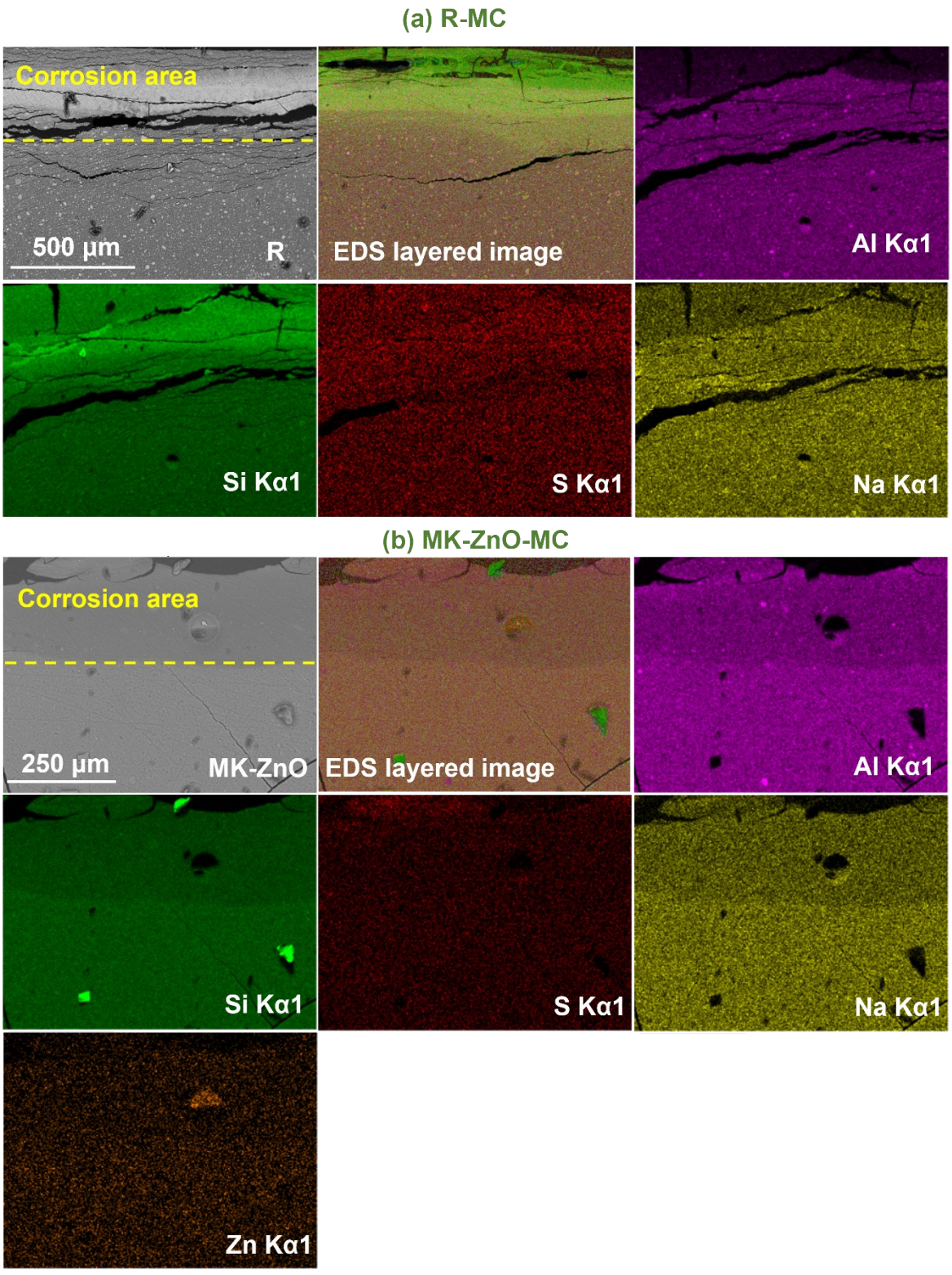

Figure S7 Results of SEM-EDS mapping of neat AAMK and ZnO-modified AAMK after 24-d microbial corrosion.